JPn Neuroscience
The Journal of Physiology



# Cholinergic modulation of the parafacial respiratory group

Rozlyn C. T. Boutin, Zaki Alsahafi and Silvia Pagliardini

*Department of Physiology, Women and Children's Health Research Institute & Neuroscience and Mental Health Institute, University of Alberta, 3020F Katz Group Centre, Edmonton, AB, T6G 2E1, Canada*

**Key points**

- This study investigates the effects of cholinergic transmission on the expiratory oscillator, the parafacial respiratory group (pFRG) in urethane anaesthetized adult rats.
- Local inhibition of the acetyl cholinesterase enzyme induced activation of expiratory abdominal muscles and active expiration.
- Local application of the cholinomimetic carbachol elicited recruitment of late expiratory neurons, expiratory abdominal muscle activity and active expiration. This effect was antagonized by local application of the muscarinic antagonists scopolamine, J104129 and 4DAMP.
- We observed distinct physiological responses between the more medial chemosensitive region of the retrotrapezoid nucleus and the more lateral region of pFRG.
- These results support the hypothesis that pFRG is under cholinergic neuromodulation and the region surrounding the facial nucleus contains a group of neurons with distinct physiological roles.

**Abstract** Active inspiration and expiration are opposing respiratory phases generated by two separate oscillators in the brainstem: inspiration driven by a neuronal network located in the preBötzinger complex (preBötC) and expiration driven by a neuronal network located in the parafacial respiratory group (pFRG). While continuous activity of the preBötC is necessary for maintaining ventilation, the pFRG behaves as a conditional expiratory oscillator, being silent in resting conditions and becoming rhythmically active in the presence of increased respiratory drive (e.g. hypoxia, hypercapnia, exercise and through release of inhibition). Recent evidence from our laboratory suggests that expiratory activity in the principal expiratory pump muscles, the abdominals, is modulated in a state-dependent fashion, frequently occurring during periods of REM sleep. We hypothesized that acetylcholine, a neurotransmitter released in wakefulness and REM sleep by mesopontine structures, contributes to the activation of pFRG neurons and thus acts to promote the recruitment of expiratory abdominal muscle activity. We investigated the stimulatory effect of cholinergic neurotransmission on pFRG activity and recruitment of active expiration *in vivo* under anaesthesia. We demonstrate that local application of the acetylcholinesterase inhibitor physostigmine into the pFRG potentiated expiratory activity. Furthermore, local application of the cholinomimetic carbachol into the pFRG activated late expiratory neurons and induced long lasting rhythmic active expiration. This effect was completely abolished by pre-application of the muscarinic antagonist scopolamine, and more selective M3 antagonists 4DAMP and J104129. We conclude that cholinergic muscarinic transmission contributes to excitation of pFRG neurons and promotes both active recruitment of abdominal muscles and active expiratory flow.

R. C. T. Boutin and Z. Alsahafi contributed equally to this work.


DOI: 10.1113/JP273012

(Resubmitted 13 July 2016; accepted after revision 28 October 2016; first published online 3 November 2016)
**Corresponding author** S. Pagliardini: 3-020F Katz Group – Rexall Centre for Health Research, Department of Physiology, Women and Children's Health Research Institute, Neuroscience and Mental Health Institute, University of Alberta, Edmonton, AB, T6G 2E1 Canada. Email: silviap@ualberta.ca

**Abbreviations** 4DAMP, 4-diphenylacetoxy-*N*-methylpiperidine methiodide; ABD, abdominal; CCh, carbachol; ChAT, choline acetyl transferase; DIA, diaphragm; GG, genioglossus; HEX, hexamethonium bromide; NeuN, neuronal nuclear marker; pFRG, parafacial respiratory group; PHYSO, physostigmine; preBötC, preBötzinger complex; PZ, pirenzepine; REM, rapid eye movement; RTN, retrotrapezoid nucleus; SCOP, scopolamine; VChaT, vesicular acetylcholine transporter.

## Introduction

Breathing is an essential behaviour for mammalian life controlled by neuronal networks located in the brainstem (Feldman *et al.* 2013). The region of the preBötzinger complex (preBötC) in the ventral medulla contains rhythmogenic neurons responsible for inspiratory rhythm generation (Smith *et al.* 1991; Feldman *et al.* 2013) while rostral to the preBötC, the region of the parafacial respiratory group (pFRG) has been proposed to be critical for expiratory rhythm generation (Janczewski *et al.* 2002; Janczewski & Feldman, 2006; Pagliardini *et al.* 2011; Huckstepp *et al.* 2015, 2016). In adult rodents, the pFRG acts as a conditional expiratory oscillator, being silent in resting conditions but rhythmically active during the expiratory phase in response to release of inhibition or direct stimulation (Pagliardini *et al.* 2011; Huckstepp *et al.* 2016). Through projections to premotoneurons in the caudal ventral respiratory group (or nucleus retroambiguus), the pFRG sends rhythmic excitatory drive to the main expiratory motoneurons and muscles, the abdominals (ABD), which then force air out of the lungs beyond their resting level (i.e. active expiration) to thereby facilitate the subsequent inspiratory phase and promote ventilation (Janczewski & Feldman, 2006; Pagliardini *et al.* 2011). Compelling evidence has shown that this pathway exists in mammals and that it is able to generate an excitatory rhythmic drive to low thoracic and lumbar motoneurons and eventually excite abdominal muscles (Boers *et al.* 2006; Janczewski & Feldman, 2006; Giraudin *et al.* 2008).

Partially overlapping with the adjacent and more ventro-medial chemosensitive region of the retrotrapezoid nucleus (RTN) (Guyenet & Bayliss, 2015), recent evidence suggests that the pFRG, which lies mostly lateral to the facial nucleus, is likely to be distinct from RTN neurons since respiratory responses to selective activation and inactivation of the two areas are different (Abbott *et al.* 2009, 2011; Pagliardini *et al.* 2011; Huckstepp *et al.* 2015). Further, the activity of RTN neurons is state-dependent, with a contribution to tidal volume unaffected by sleep states, and little contribution to respiratory frequency and active expiration observed in rapid eye movement (REM) sleep compared to more potent respiratory effects observed in wakefulness and non-REM sleep (Burke *et al.* 2015).

We recently reported that recruitment of expiratory ABD muscle activity in adult rats frequently occurs during periods of REM in natural sleep and in REM-like states under urethane anaesthesia (Pagliardini *et al.* 2012, 2013; Andrews & Pagliardini, 2015). Moreover, this recruitment leads to increased respiratory stability and increased tidal volume and minute ventilation (Andrews & Pagliardini, 2015). Currently, the source of rhythmic excitatory drive to ABD muscles in REM sleep is unknown. Given the proposed role of pFRG neurons in promoting expiratory activity in ABD muscles, in generating active expiration (Janczewski & Feldman, 2006; Pagliardini *et al.* 2011), and in interacting with preBötC to pace respiratory rhythms (Mellen *et al.* 2003; Janczewski & Feldman, 2006; Pagliardini *et al.* 2011; Huckstepp *et al.* 2016), one possibility is that pFRG neurons become rhythmically active during REM sleep (either through release of inhibition (Pagliardini *et al.* 2011) or through incoming excitatory inputs) to provide an excitatory rhythmic drive to ABD muscles.

In this study, we tested the hypothesis that cholinergic transmission, which is potentiated in periods of REM sleep in the reticular formation from its ascending and descending sources in the brainstem (Kodama *et al.* 1992), is involved in the modulation of pFRG neurons and generation of active expiratory activity in urethane anaesthetized rats.

Immunohistological results suggest that the pFRG region contains cholinergic fibres and terminals. In addition, local application of the acetylcholinesterase enzyme inhibitor physostigmine promoted recruitment of $ABD_{EMG}$ activity as well as an increase in tidal volume and minute ventilation. Similarly, local application of the cholinomimetic agent carbachol (CCh) into the pFRG induced potent recruitment of $ABD_{EMG}$ activity, expiratory flow, and an increase in both tidal volume and minute ventilation. The effects induced by CCh were completely inhibited by pre-application of the muscarinic antagonist scopolamine (SCOP) and strongly inhibited by more selective M3 muscarinic antagonists 4-diphenylacetoxy-*N*-methylpiperidine methiodide (4DAMP) and J104129.

Within the same region of the ventral surface of the medulla, chemosensitive neurons of the RTN have been identified and characterized (Guyenet & Bayliss, 2015). Currently, it is still debated if expiratory rhythmogenic pFRG neurons represent a separate neuronal group from the more chemosensitive neurons in RTN. In order to further distinguish between respiratory responses elicited by the medial and lateral regions surrounding the facial nucleus (i.e. lateral pFRG *vs.* medial RTN) we tested respiratory effects induced by local application of CCh in the two areas. While both regions produced active recruitment of ABD muscles, we observed a difference in the resulting respiratory frequency response between the two sites, further supporting the hypothesis of a distinct respiratory function for the medial and lateral parafacial regions.

In summary, these results demonstrate that cholinergic muscarinic transmission contributes to excitation of pFRG neurons and promotes active recruitment of $ABD_{EMG}$ activity and active expiratory flow, thereby acting as a potential mechanism by which state-dependent control during REM could take place.

## Methods

### Ethical approval

Animal handling and experimental protocols were approved by the Health Science Animal Policy and Welfare Committee of the University of Alberta according to the guidelines established by the Canadian Council on Animal Care, and they are in compliance with the guidelines of *The Journal of Physiology* (Grundy, 2015).

### Immunohistochemistry

Immunohistochemistry was performed according to previously published protocols (Pagliardini *et al.* 2003, 2011). Eight adult male rats were anaesthetized with urethane (I.P., 2 g $kg^{-1}$) and transcardially perfused with 4% paraformaldehyde dissolved in phosphate buffer (PB). The brains were collected, post-fixed, and 50 $\mu$m brainstem transverse sections were cut with a VT1000 vibrating blade microtome (Leica, Wetzlar, Germany). Free-floating sections were rinsed in phosphate-buffered saline (PBS) and incubated with 10% normal donkey antiserum (NDS) and 0.3% Triton X-100 for 60 min to reduce non-specific staining and increase antibody penetration. Sections were then incubated overnight with primary antibodies diluted in PBS containing 1% NDS and 0.3% Triton X-100. The following day, sections were washed in PBS, incubated with the specific secondary antibodies conjugated to the fluorescent probes (Cy3-conjugated anti-goat; Cy2/Cy5-conjugated anti-mouse; Jackson ImmunoResearch Laboratories, West Grove, PA, USA) diluted in 1% NDS and PBS for 2 h. Sections were further washed in PBS, mounted and coverslipped with Fluorsave mounting medium (Calbiochem, Billerica, MA, USA). The primary antibodies used for this study detected the following proteins: neuronal nuclear marker (NeuN; raised in mouse; Millipore, 1:500), vesicular acetylcholine transporter (VChaT; raised in in goat; Millipore, 1:1000), choline acetyl transferase (ChAT; raised in goat; Millipore, 1:500). Slides were then observed under a LSM512 Zeiss confocal microscope. Images of the pFRG, the RTN and the adjacent facial nucleus were acquired, exported as TIFF files and arranged to prepare final figures.

### Acute experimental procedures

A total of 71 adult male Sprague–Dawley rats (280–350 g) were used for acute experiments. Rats were initially anaesthetized in isofluorane (2% in air) while the femoral vein was cannulated and urethane (1.5 g (kg body weight)$^{-1}$) was gradually delivered to induce permanent and irreversible anaesthesia. Additional doses of anaesthesia were delivered as necessary to maintain a surgical plane of anaesthesia. The trachea was cannulated and respiratory flow was detected with a flow head connected to a transducer (GM Instruments, Kilwinning, UK). Coupled EMG wire electrodes (CoonerWire, Chatsworth, CA, USA) were inserted into the genioglossal (GG), oblique abdominal (ABD) and diaphragm (DIA) muscles. Wires were connected to amplifiers (AM Systems, Carlsborg, WA, USA) and activity was sampled at 2 kHz (Powerlab 16/30; ADInstruments, Colorado Springs, CO, USA). Rats were vagotomized by resecting a portion of the vagus nerve (2 mm) at the mid-cervical level and body temperature was kept constant at 37 $\pm$ 1°C with a servo-controlled heating pad (Harvard Apparatus, Holliston, MA, USA). In order to reduce tracheal secretion, scopolamine 3-methylbromide (0.1 ml per 100 g) was often injected subcutaneously at the beginning of the experiment.

In rats where EEG activity was monitored, Teflon-coated stainless steel wires (AM-Systems, Inc., Carlsborg, WA, USA) were implanted in the neocortex (nCTX) and hippocampal formation (HPC) according to the following coordinates relative to bregma: nCTX: anterior-posterior (AP): +2.5; mediolateral (ML): −1.2; dorsoventral (DV): −1.5 to −2.0 mm. HPC: AP, −3.3; ML, −2.4; DV, −2.5 to −3.0 mm). Electrodes were then fixed to the skull by jeweler's screws and dental acrylic. Anaesthetized and instrumented rats were then positioned on the stereotaxic frame with bregma 5 mm below lambda. Physostigmine (PHYSO, 5 mM, 200 nl), carbachol (CCh, 1–10 mM, 50–100 nl), scopolamine (SCOP; 10 mM, 200 nl), pirenzepine (PZ; 1–10 mM, 100 nl), 4-diphenylacetoxy-N-methylpiperidine

methiodide (4DAMP; 1 mM, 100 nl), J104129 (1–10 mM, 100 nl), AF-DX-116 (1 mM, 100 nl) and hexametonium bromide (HEX; 1-10 mM, 100 nl) diluted in Hepes buffer (Gourine *et al.* 2010) were pressure injected through a sharp glass electrode (30 $\mu$m tip diameter) into the pFRG. Fluorescent beads (200 nm diameter, 0.1–1%, Invitrogen, Carlsbad, CA, USA) were added to the injected solution to locate the injection site. Stereotaxic coordinates for injections into the pFRG were (in mm) AP, +1.8, ML, ±2.5 and DV, −3.4–3.5 relative to the obex. Stereotaxic coordinates for injections into the RTN were (in mm) AP, +1.8–2.1, ML, ±1.8 and DV, −3.5–3.6 relative to the obex. Control experiments were performed by injecting Hepes buffer (vehicle; 50–200 nl) solution in the same locations.

### Unit recordings

In eight experiments we recorded multi-unit activity within the pFRG after local application of CCh. Anaesthetized rats positioned on the stereotaxic frame received a bilateral microinjection of CCh (10 mM, 200 nl); once active recruitment of expiratory ABD muscle activity was observed, a 12 mΩ tungsten electrode (AM Systems) was connected with a One Axis IVM Scientifica micromanipulator and units were recorded at stereotaxic coordinates (in mm) 1.8 rostral, 2.4–2.5 lateral and 3.4–3.5 ventral to the obex. Localization of the electrode was confirmed by histological examination of post-fixed tissue.

### Histology

At the end of each experiment, rats were transcardially perfused with 4% paraformaldehyde dissolved in PB. The brains were collected, post-fixed, and 50 $\mu$m thick serial transverse sections were either directly mounted on slides and coverslipped for detection of fluorescent beads (i.e. injection site) or counterstained with thionine for identification of brainstem cyto-architecture. Slides were coverslipped and observed under a Leica DM5500B fluorescence microscope to locate injection sites. Images were acquired with Metamorph (Molecular Devices, Sunnyvale, CA, USA) program, exported as TIFF files and arranged to identify rostro-caudal and mediolateral coordinates of injection sites, electrode placement (referenced to the Paxinos rat brain atlas), and to prepare final figures.

### Data analysis

Signals from EMG electrodes were amplified at ×10,000, filtered between 300 Hz and 1 kHz. Field potential activity from nCTX and HPC was amplified at ×1,000, and filtered between 0.1 Hz and 500 Hz. Data were sampled at 2 kHz with a PowerLab 16/35 acquisition system. Field Unit activity was amplified at ×10,000, filtered between 100 Hz and 10 kHz, and sampled at 10 kHz. Data were then analysed using LabChart7 Pro (ADInstruments), Excel 2013 and Origin 9 (OriginLab Corp., Northampton, MA, USA) software. The absolute value of EMG signals was digitally rectified and integrated with a time constant of 0.08 s to calculate peak amplitude. Baseline activity was averaged over 5 min before drug injection and normalized. Respiratory changes upon drugs application are indicated as percentage change compared to baseline values. The respiratory airflow signal was used to calculate respiratory rate, tidal volume and minute ventilation. Tidal volume was obtained by integration of airflow amplitude and converted to millilitres of air by comparison with a five-point calibration curve (0.5–5 ml range). Statistical significance of respiratory changes before and during drug injection was tested with Student's paired *t* test, with threshold for significance set at 0.05. Effects of muscarinic antagonists on $ABD_{EMG}$ recruitment were evaluated by comparing $ABD_{EMG}$ peak amplitude activity following CCh injection and subsequent combined CCh and muscarinic antagonist injections in addition to comparing combined CCh and muscarinic antagonist injections with CCh repeated measures, as illustrated in figure 7D. For experiments that compared medial and lateral injections, changes in physiological parameters were compared to pre-injection values and data are reported as percentage change in both conditions. Data are reported as mean ± standard error of the mean.

## Results

### Cholinergic innervation is present in, and localized to, the pFRG region

In order to investigate the presence of endogenous cholinergic innervation in the region of the pFRG, coronal brainstem sections were immunolabelled for choline acetyltransferase (ChAT) and vesicular acetylcholine transporter (VChaT), two markers that respectively identify cholinergic fibres and terminals in the region surrounding the facial nucleus (Fig. 1). Labelling of fibres and cholinergic terminals was observed lateral to the caudal edge of the facial nucleus, at the level of the injection sites depicted in Figs 5 and 8. Figure 1 displays expression of VChaT positive presynaptic terminals in the region surrounding the caudal tip of the facial nucleus, both medial (the region corresponding to the chemosensitive area of the RTN) and lateral to the facial nucleus (the region corresponding to the pFRG) (Pagliardini *et al.* 2011; Huckstepp *et al.* 2015). Within the pFRG, we observed several VChaT positive puncta in close contact with neurons located lateral to the caudal tip of the facial nucleus (Fig. 1*D*), the site of injection of CCh and putative location of the pFRG (Pagliardini *et al.* 2011; Huckstepp *et al.* 2015). Within RTN we were also able to identify

several VChaT positive puncta (Fig. 1*B*). More rostrally (> 400 $\mu$m from the caudal tip of the facial nucleus), staining for ChAT and VChaT was limited to the area of the facial nucleus in the ventral brainstem. These results support the hypothesis that cholinergic innervation is present in this area and may influence pFRG activity.

### Inhibition of endogenous acetylcholinesterases in the pFRG increases abdominal expiratory activity

We then tested the hypothesis that endogenous acetylcholine (ACh) affects rhythmic activity of pFRG neurons and consequently promotes expiratory modulated activity of ABD muscles. We locally applied an inhibitor of the acetylcholinesterase enzyme (physostigmine, PHYSO, 5 mM, 200 nl) that blocks degradation of ACh and therefore progressively increases endogenous ACh levels within the pFRG. Bilateral local PHYSO application into the pFRG gradually increased tonic $ABD_{EMG}$ activity until it maximally developed within 2.0 ± 0.6 min and lasted for 13.2 ± 0.5 min ($n$ = 8; Fig. 2*A*). In addition to potentiating expiratory $ABD_{EMG}$ activity (202 ± 58% increase in expiration compared to $ABD_{EMG}$ activity during the preceding inspiration, $P = 6.3 \times 10^{-4}$; $n$ = 8; 285 ± 115% increase in expiration compared to pre-injection values, $P$ = 0.019; $n$ = 8), peak inspiratory $\int DIA_{EMG}$ activity increased by 26.0 ± 17.2% ($P = 6.8 \times 10^{-4}$; $n$ = 8), peak $\int GG$ activity increased by 64.8 ± 46.2% ($P$ = 0.021; $n$ = 5), and tidal volume increased by 22.8 ± 5.5% ($P = 5.5 \times 10^{-4}$; $n$ = 8; Fig. 2*C*) compared to pre-injection values. In four experiments potentiation of inspiratory EMG activity shortly preceded recruitment of ABD activity, while in the remaining experiments, potentiation in the investigated muscles occurred at the same time. Respiratory frequency decreased from 51.2 ± 3.3 to 44.4 ± 2.3 breaths per minute (bpm; $P = 1.7 \times 10^{-3}$; $n$ = 8) compared to control. As a consequence, minute ventilation was only marginally increased (+9.2 ± 5.1%; $P$ = 0.043; $n$ = 8). In 6 out of 8 experiments, PHYSO-induced $ABD_{EMG}$ recruitment was sufficient to generated active expiration (i.e. negative deflection in airflow in late expiration; Fig. 2*B*).

In order to verify that ABD activation was not dependent on a potential brain activation state, we recorded hippocampal/cortical EEG activity in a subset of animals ($n$ = 6; Fig. 3*A* and *B*). Infusions of PHYSO did not alter ongoing spontaneous brain alternations, but onset of ABD recruitment occurred most frequently with onset of the activated state (Fig. 3*B*). Furthermore, the occurrence of ABD recruitment outlasted the ongoing alternations into activated (theta) states by an average of 2.0 ± 0.8 min ($n$ = 6; Fig. 3*A*). These results indicate that the effects on ABD activity were dependent on local inhibition of degradation of ACh within the pFRG occurring at the onset or during an activated state and not on the induction of a generalized activated brain state.

### Activation of cholinergic receptors in pFRG recruits abdominal expiratory activity and active expiration

We tested the hypothesis that cholinergic neurotransmission is involved in the recruitment of rhythmic activation of the expiratory oscillator in the pFRG. Local bilateral application of carbachol (CCh, 10 mM, 100 nl) into the pFRG generated strong recruitment of active expiration ($n$ = 11; Fig. 4*A*). The cholinergic agonist CCh induced an initial activation of tonic expiratory activity in the ABD muscles (46.3 ± 12.6 s delay from the first CCh injection), promptly followed by recruitment of potent phasic expiratory activity upon bilateral injection that lasted for 14.92 ± 1.93 min ($n$ = 11). During this time, respiratory frequency decreased from 49.3 ± 1.5 to 41.6 ± 2.1 bpm ($P = 3 \times 10^{-5}$; $n$ = 11), peak inspiratory $\int DIA_{EMG}$ activity increased by 46.8 ± 20.3% ($P$ = 0.01; $n$ = 11) and peak $\int GG$ activity increased by 109.7 ± 35.7% ($P = 7.9 \times 10^{-4}$; $n$ = 11; Fig. 4*C*). Integrated $ABD_{EMG}$ activity before CCh injection displayed either a tonic activity through the respiratory cycle ($n$ = 8) or

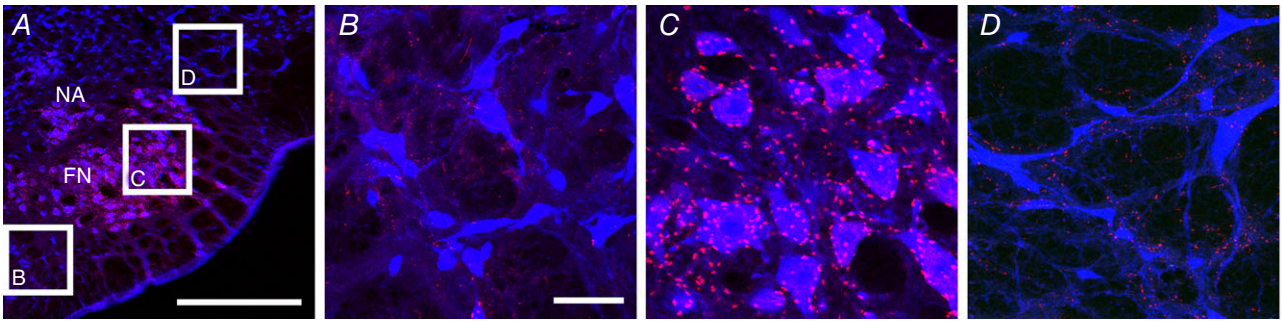


**Figure 1. Distribution of cholinergic terminals in the parafacial area**
*A*, low magnification image of the parafacial area immunoreacted for NeuN (blue) and VChaT (red). Boxes in *A* indicate the areas where images corresponding to the retrotrapezoid nucleus (*B*), facial nucles (*C*) and pFRG (*D*) have been acquired. Note the presence of fine VChaT positive puncta in both pFRG and RTN areas. Calibration bars: *A*: 500 $\mu$m, *B–D*: 50 $\mu$m.

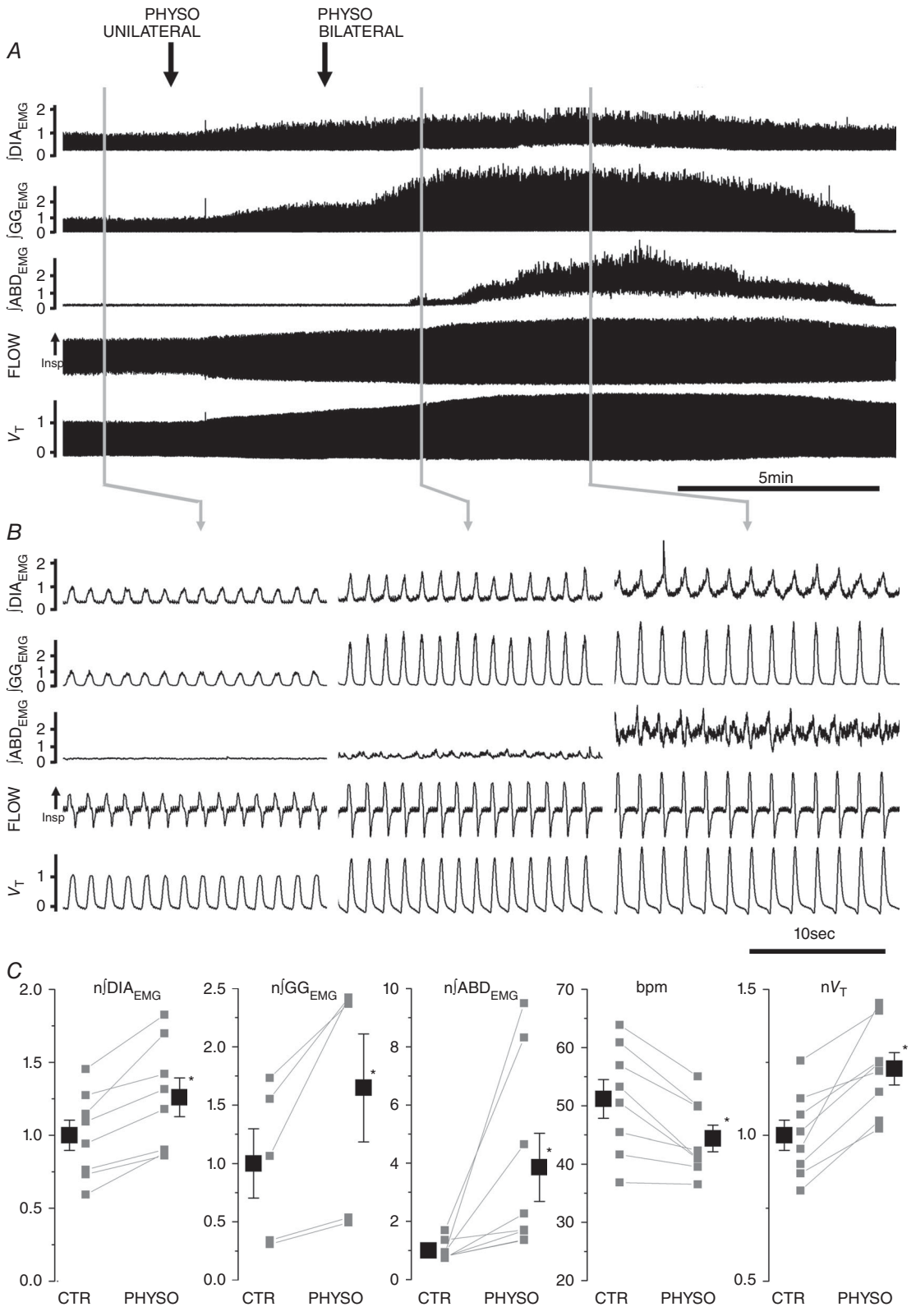


**Figure 2. Local application of physostigmine (PHYSO, 5 mm, 200 nl) in pFRG induces long lasting ABD recruitment and active expiration**

*A*, long trace recordings of $\int DIA_{EMG}$, $\int GG_{EMG}$ and $\int ABD_{EMG}$, respiratory airflow and tidal volume ($V_T$) during local bilateral application of PHYSO (black arrows indicate time of injections on the two sides of the ventrolateral medulla). *B*, details of respiratory traces before (left) and after PHYSO application (centre and right). Note

progressive activation of expiratory modulated $ABD_{EMG}$ activity. *C*, single experiment data (grey) and averaged data (black) on the effect of bilateral application of PHYSO on $\int DIA_{EMG}$, $\int GG_{EMG}$ and $\int ABD_{EMG}$, breaths per minute (bpm) and tidal volume ($V_T$). EMG and tidal volume data are normalized (n) to control values (CTR) and asterisks indicate statistical significance ($P < 0.05$) relative to pre-injection CTR values.

a weak expiratory modulated activity ($n = 3$). In both cases, $ABD_{EMG}$ activity increased during inspiration by $21.2 \pm 8.9\%$ compared to pre-injection values ($P = 0.02$; $n = 11$) and activity during expiration displayed a peak in late expiration that was $176 \pm 33\%$ larger compared to pre-injection values ($P = 1.2 \times 10^{-5}$) and a $123 \pm 16\%$ increase compared to $ABD_{EMG}$ activity during the preceding inspiration ($P = 1.3 \times 10^{-7}$). Activation of ABD muscles occurred either in synchrony with potentiation of DIA and $GG_{EMG}$ activity (6/11) or followed shortly

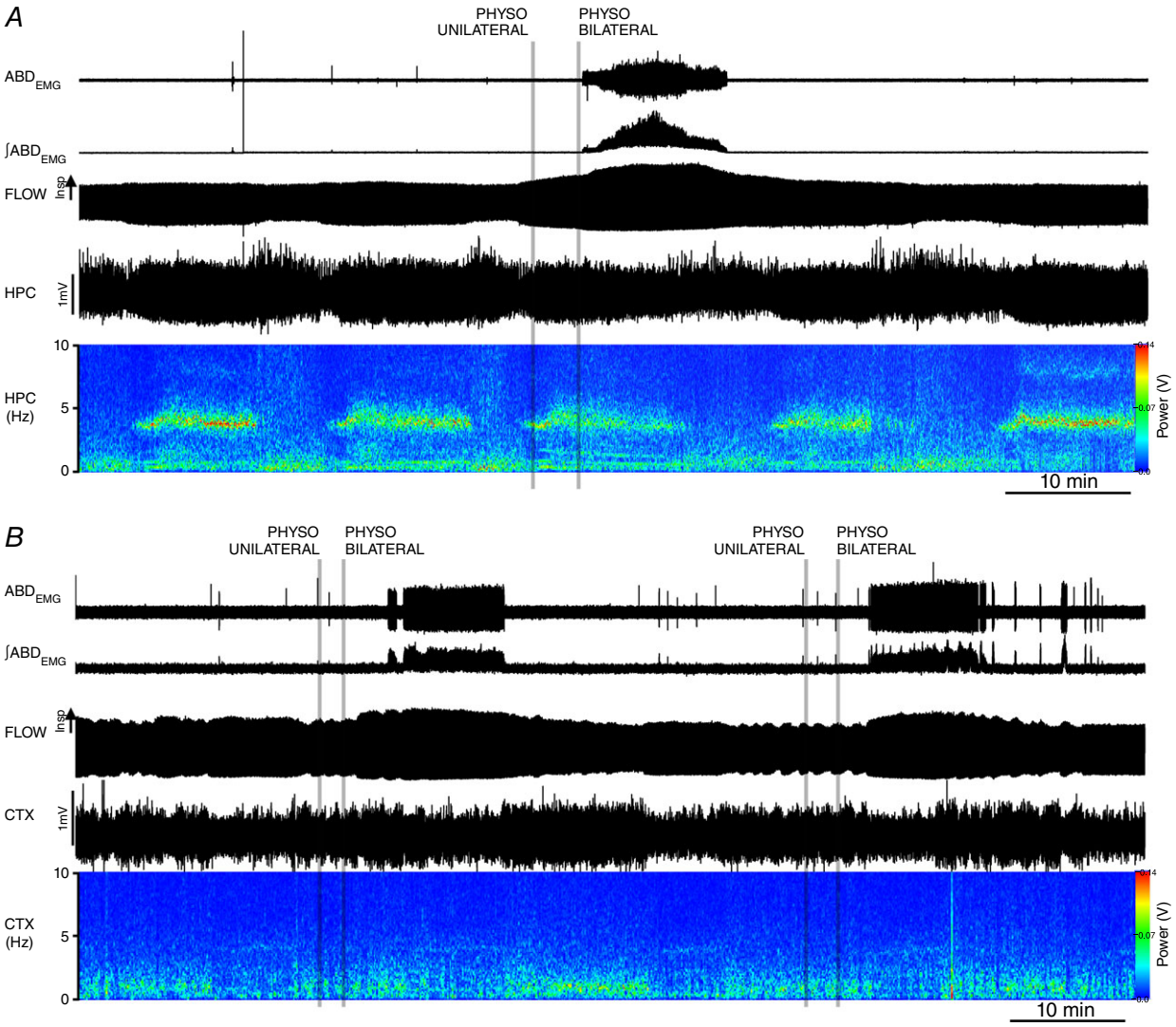


**Figure 3. Local application of physostigmine (PHYSO, 5 mm, 200 nl) in pFRG does not affect spontaneous brain state alternations**
*A*, long trace recordings of $ABD_{EMG}$, $\int ABD_{EMG}$, respiratory airflow, hippocampal activity (HPC) and its power spectrogram during local bilateral application of PHYSO (grey lines indicate time of injections on the two sides of the ventrolateral medulla) during activated state (high power at 4 Hz frequency). Note lack of effect in spontaneous brain state alternation and the persistence of expiratory activity with brain state changes. *B*, long trace recordings of $ABD_{EMG}$, $\int ABD_{EMG}$, respiratory airflow, cortical activity (CTX) and its power spectrogram during local bilateral application of PHYSO during deactivated state (high power at 1 Hz frequency). Note lack of effect in spontaneous brain state alternation and the onset of expiratory activity occurring with activated states (i.e., low power in the CTX 1 Hz frequency range).

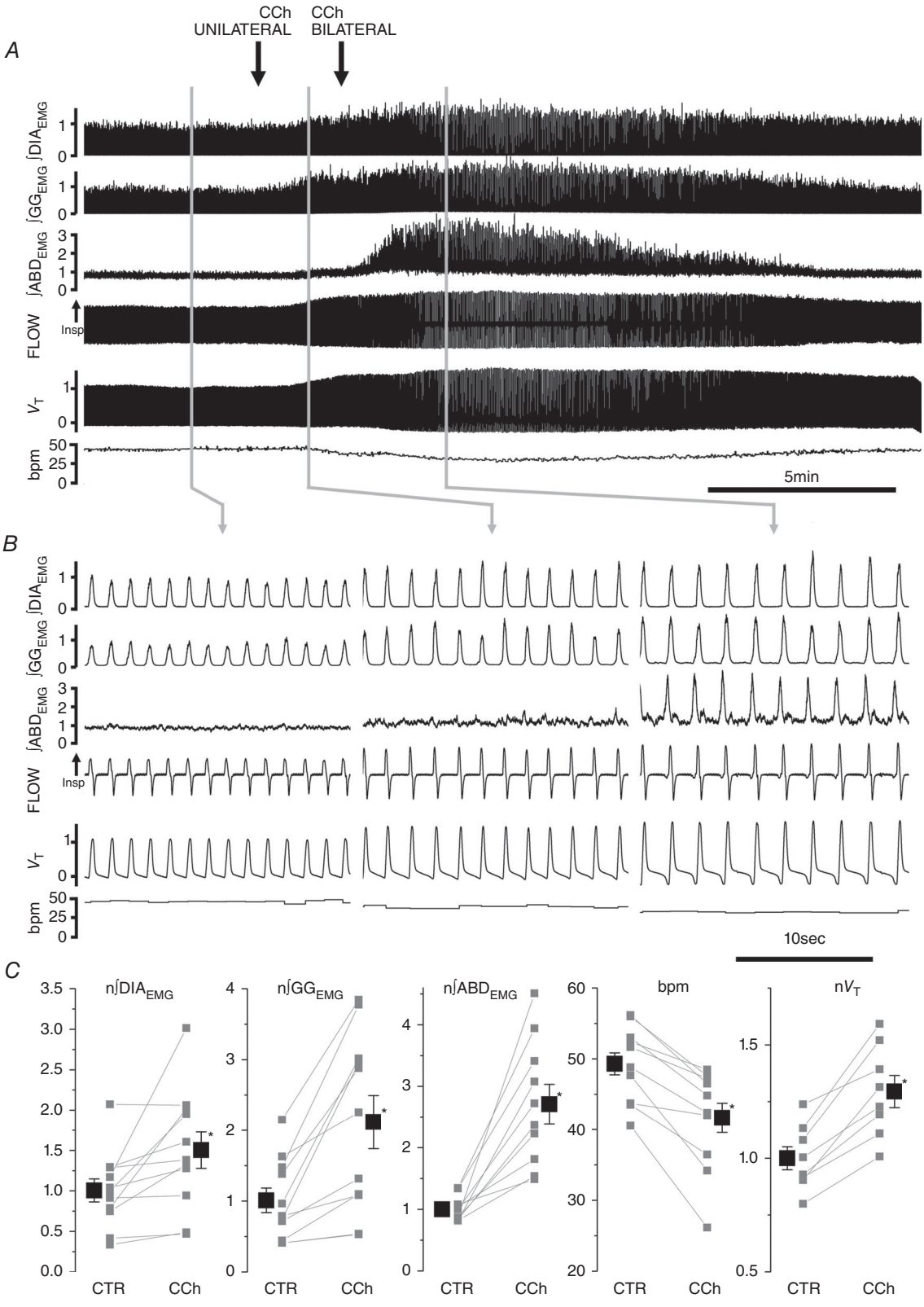


**Figure 4. Local application of carbachol (CCh, 10 mm, 100 nl) in pFRG induces long lasting ABD recruitment and active expiration**
*A*, effect of bilateral application of CCh on $\int DIA_{EMG}$, $\int GG_{EMG}$ and $\int ABD_{EMG}$, respiratory airflow, tidal volume ($V_T$), and respiratory rate (bpm). Black arrows indicate time of injections. *B*, details of respiratory traces before (left), following the first (unilateral, centre) and second (bilateral, right) CCh injections into the pFRG of urethane

anaesthetized rats. Note progressive activation of expiratory modulated $ABD_{EMG}$ activity following CCh injection. *C*, single experiment (grey) and averaged data results (black) on the effect of bilateral application of CCh on $\int DIA_{EMG}$, $\int GG_{EMG}$ and $\int ABD_{EMG}$, breaths per minute (bpm) and tidal volume ($V_T$). Respiratory muscle EMGs and tidal volume data are normalized to control and asterisks indicate statistical significance ($P < 0.05$) relative to pre-injection control values.

after their activation (5/11). As a consequence of pFRG activation by CCh, tidal volume increased by 29.4± 6.7% ($P = 1.3 \times 10^{-4}$; $n = 9$) and minute ventilation increased by 9.9 ± 3.0% ($P = 9 \times 10^{-3}$; $n = 9$). A strong recruitment of $ABD_{EMG}$ activity and active expiration was consistently observed when injection was positioned around the lateral caudal tip of the facial nucleus. Injection sites are indicated in Fig. 5.

Furthermore, similar to PHYSO experiments, infusions of CCh into the pFRG did not significantly alter ongoing spontaneous brain alternations ($n = 6$) and occurrence of ABD recruitment was not associated with brain state alternations.

### Activation of late expiratory activity neurons within pFRG during carbachol stimulation

In eight experiments we recorded multi-unit activity from the region of pFRG upon local microinjection of CCh and recruitment of active expiration. In this region we were able to identify expiratory modulated neurons ($n = 8$ in 8 rats), inspiratory neurons ($n = 5$), and tonic neurons ($n = 10$). In addition, after CCh application into the pFRG, we identified units with a clear discharge during late expiration ($n = 11$ in 8 rats; Fig. 6*A*); these units were in phase with the peak of $ABD_{EMG}$ activity and became silent upon waning of the CCh-induced expiratory effect. These results suggest that neurons with a late expiratory phenotype are localized within the pFRG region, they are silent in resting conditions, but are likely to be activated by local CCh application (Fig. 6*B*).

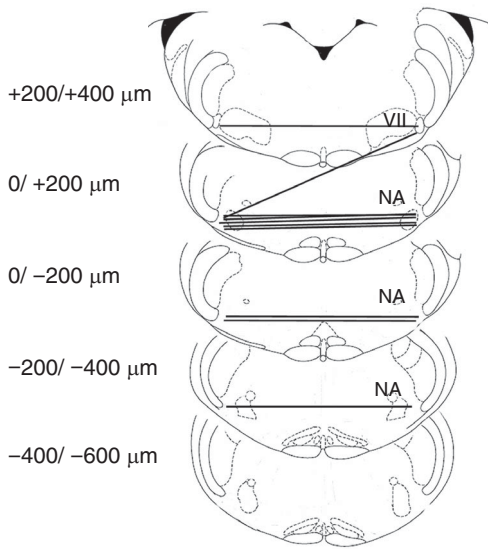


**Figure 5. Effective CCh injection sites are localized in the pFRG area**
Representative sections of adult rat brainstem indicating CCh injection sites in the pFRG of urethane anaesthetized rats that promoted recruitment of ABD activity and active expiration (modified from Paxinos and Watson, 1998); 0 $\mu$m corresponds to the caudal tip of facial nucleus (VII). Each symbol represents an injection site and lines connect the two injection sites performed in each experiment ($n = 10$). NA: nucleus ambiguus.

### Activation of pFRG is antagonized by scopolamine and M3 receptor antagonists

We further tested the hypothesis that the cholinergic effect on pFRG neurons is mediated by muscarinic receptors by determining if application of muscarinic antagonists blocks CCh-induced recruitment of $ABD_{EMG}$ activity and active expiration. In seven experiments, after confirmation that CCh injections (10 mM, 100 nl) into the pFRG successfully induced active expiration and a complete washout of the CCh effect (~60 min), we bilaterally injected scopolamine (SCOP, 10 mM 200 nl) shortly followed by a second CCh injection (~5 min; Fig. 7*A*). SCOP, a wide spectrum muscarinic receptor antagonist, completely blocked CCh-induced recruitment of $ABD_{EMG}$ activity ($P = 0.3$), changes in $DIA_{EMG}$ activity ($P = 0.99$), $GG_{EMG}$ activity ($P = 0.91$), tidal volume ($P = 0.3$) and respiratory frequency ($P = 0.3$; $n = 7$; Fig. 7*B*). Interestingly, prior to SCOP injection, three out of seven rats displayed weak expiratory related activity (Fig. 7*A*) that was eliminated by injection of SCOP in the pFRG. Application of CCh within 5 min from SCOP application did not induce expiratory $ABD_{EMG}$ activity or active expiration or cause any significant respiratory change.

Recovery from SCOP injection (i.e. CCh-induced $ABD_{EMG}$ activation) was tested at 1 and 2 h after injection and active expiration was successfully observed only after 2 h from SCOP injection ($n = 3/3$; Fig. 7*A*). Verification of injection sites was performed by identification of fluorescent beads added to the drug and vehicle solutions (534 red beads for CCh injections and 488 green beads for SCOP injection) as displayed in Fig. 7*C*.

To further identify the muscarinic receptor subtype involved in the CCh-induced generation of active expiration, we co-applied CCh with a variety of antagonists having different profiles of affinity for the M1, M2 and M3 receptors. In particular, we used pirenzepine (PZ: M1 > M3), AF-DX116

(M2) as well as 4-diphenylacetoxy-*N*-methylpiperidine methiodide (4DAMP) and J104129 (M3 > M1). For each, we compared the responses obtained after a first application of CCh (10 mM, 100 nl) alone to those with a subsequent (repeated) application of CCh combined with each antagonist (Fig. 7*D*). To ensure that any decreases reported were not simply due to receptor desensitization, we conducted control experiments in which we made repeated applications of CCh and compared the effects of antagonists to the average decrease. Repeated applications of CCh alone into pFRG evoked an $ABD_{EMG}$ response that was 86.0 ± 4.0% of its initial response ($n = 6$; $P = 9.0 \times 10^{-3}$). The M2 selective antagonist AF-DX116 displayed a small but significant reduction in blocking ABD recruitment compared to the initial maximal response (75.7 ± 3.8%; $P = 4 \times 10^{-3}$; $n = 4$) but no significant change compared to repeated CCh application ($P = 0.11$). 4DAMP, an antagonist that is more selective for M3 and M1 but has very low affinity for M2 receptors, was able to reduce ABD recruitment to 35.6 ± 11.5% ($P = 0.006$; $n = 4$) of the initial maximal response, and to 41.2 ± 7.2% of the response to a repeated application of CCh ($P = 9.5 \times 10^{-5}$). The results suggest that M1/M3 subtypes are likely to be involved in the CCh-induced ABD recruitment.

Application of a more selective M3 antagonist, J104129, at equimolar concentrations was able to reduce ABD recruitment to 36.2 ± 5.3% ($P = 0.001$; $n = 4$) of the initial maximal response and to 42.0 ± 7.4% of the repeated application of CCh ($P = 1.1 \times 10^{-4}$). Injection of the more selective M1 antagonist PZ reduced ABD recruitment only to 70.5 ± 11.9% ($P = 0.045$; $n = 4$) of the initial maximal response but showed no significant change compared to a repeated CCh application ($P = 0.18$). When a 10-fold higher concentration of PZ was tested (10 mM), ABD recruitment was reduced to 32.3 ± 12.2% ($P = 5.7 \times 10^{-3}$; $n = 4$) of the initial maximal response. Given the similar $K_i$ of J104129 and PZ for human M1 receptors ($K_i = 19$ nM and 16 nM, respectively) and the reduced selectivity of PZ for M1 *versus* M3 compared to J104129, we attribute the high-dose effect of PZ to inhibition of M3 receptors.

Notwithstanding the limitation of these experiments due to lack of highly specific muscarinic agonists and antagonists currently available, we conclude that M3 receptors are the most likely receptor subtype responsible for CCh-induced generation of active expiration.

To exclude possible contributions of nicotinic receptors to CCh within the pFRG, we also applied a wide spectrum nicotinic receptor antagonist, hexametonium bromide (HEX), into the pFRG. Co-application of both 1 mM and 10 mM HEX did not affect ABD recruitment compared to the initial maximal response ($P = 0.3$ and $P = 0.25$, respectively; $n = 4$). These results suggest that nicotinic receptors have no effect on pFRG activation and ABD recruitment.

## CCh response in the medial and lateral regions surrounding the facial nucleus

Previous work has shown that the chemosensitive area medial and ventral to the facial nucleus, corresponding to the RTN, displays an excitatory response to local application of cholinergic agonists (Dev & Loeschcke, 1979; Nattie & Li, 1990). An ongoing issue in respiratory neurophysiology is related to the identity of pFRG neurons and the possibility of their being a distinct class of respiratory neurons from the adjacent RTN neurons.

In order to further test the hypothesis that regions medial and lateral to the ventral surface of the facial nucleus correspond to functionally different structures involved in respiratory control, namely RTN (medially) and pFRG (laterally), we injected a smaller volume and a lower concentration of CCh (50 nl, 1 mM) at 1.8 and 2.5 mm from the midline, with the objective of identifying

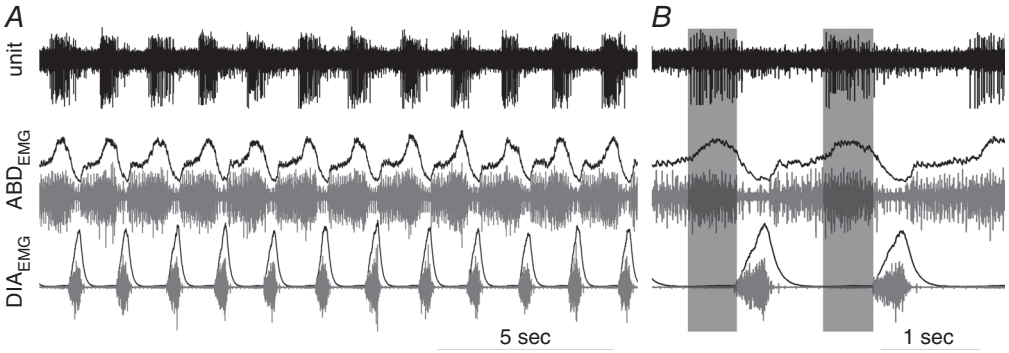


**Figure 6. Late expiratory neurons are located at the site of CCh injection during recruitment of active expiration**
Multiunit activity recorded at injection site, integrated (black) and raw (grey) $DIA_{EMG}$ and $ABD_{EMG}$ activity recorded during expression of active expiration induced by local microinjection of CCh into the pFRG. *A*, long trace recording; *B*, detail of multiunit activity across two respiratory events.

local differences in the physiological response to CCh between the two areas (Fig. 8*A*). CCh injection in the lateral pFRG caused respiratory rate depression compared to pre-injection values ($-27.1 \pm 3.1\%$; $P = 7.7 \times 10^{-6}$; $n = 11$; pre-injection values were compared to the maximal respiratory frequency response following injection). On the other hand, CCh injections medial to the facial nucleus increased the respiratory rate by $21.0 \pm 5.2\%$ compared to pre-injection values ($P = 7.2 \times 10^{-4}$; $n = 11$). The change in respiratory rate response between medial and lateral injections was significant ($P = 3.9 \times 10^{-6}$). CCh injections increased peak inspiratory $\int DIA_{EMG}$ activity in both lateral ($+41.6 \pm 12.1\%$; $P = 0.002$) and medial ($+19.2 \pm 5.6\%$; $P = 0.003$) injection sites. In addition, upon CCh injection tidal volume ($V_T$) was increased in both lateral ($+28.3 \pm 4.9\%$; $P = 3.9 \times 10^{-4}$) and medial ($+12.8 \pm 2.7\%$; $P = 3.0 \times 10^{-4}$) injection sites as well as minute ventilation ($+11.0 \pm 4.8\%$, $P = 0.01$ in lateral injections; $+20.6 \pm 5.0$, $P = 0.001$ in medial injections). Again, comparison between lateral and medial injections

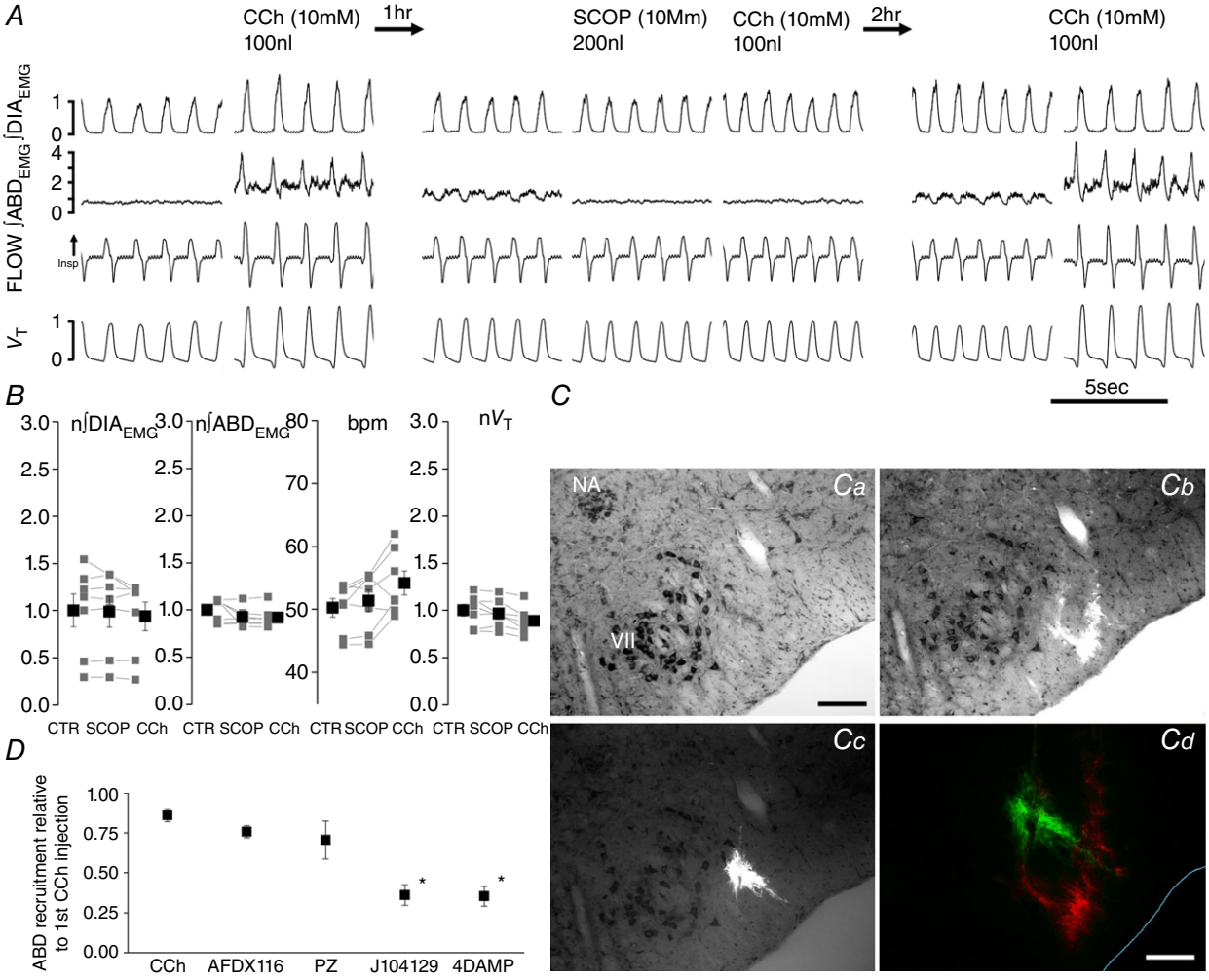


**Figure 7. Scopolamine blocks CCh induced recruitment of $ABD_{EMG}$ and active expiration**
*A*, details of traces from $\int DIA_{EMG}$, $\int ABD_{EMG}$, respiratory flow and tidal volume ($V_T$) before and after first CCh injection (left), before and after SCOP and CCh (centre), and CCh injection after the recovery period (right). *B*, effect of bilateral application of SCOP followed by CCh injection on normalized $\int DIA_{EMG}$ and $\int ABD_{EMG}$, bpm and normalized tidal volume ($V_T$). Note lack of significant changes on respiratory parameters ($P > 0.05$) after SCOP and CCh injection relative to pre-injection control values (grey, individual experiments; black, averaged data). *C*, images taken from a transverse section at the caudal tip of the facial nucleus counterstained with thionine (*a*) and illustrating multiple injection sites for CCh (*b*) and injection site for SCOP (*c*); *d* illustrate proximity of injections of the two drugs (SCOP, green; CCh, red). *D*, effects of the muscarinic antagonists AF-DX116, PZ, J104129 and 4DAMP on CCh-induced $ABD_{EMG}$ activity. Data are reported as relative to initial (first injection) CCh-induced contraction of ABD muscles calculated in the first 5 min post-injection. Significant changes relative to second CCh injection are indicated with an asterisk. Calibration bar C*a*–*c*: 200 $\mu$m; C*d*: 100 $\mu$m. NA, nucleus ambiguus; VII, facial nucleus.

indicated significant differences in the ratio of change for $V_T$ ($P = 5.9 \times 10^{-3}$) and minute ventilation ($P = 0.03$) but no significant difference in change of $\int DIA_{EMG}$ peak amplitude ($P = 0.06$) between the two sites (Fig. 8*B*).

In seven out of eleven experiments local bilateral application of 1 mM CCh into the lateral pFRG generated strong recruitment of abdominal muscles. In the remaining four experiments, although we observed respiratory rate depression and changes in tidal volume, excitation was not sufficient to induce $ABD_{EMG}$ recruitment and active expiration. Overall, $ABD_{EMG}$ activity increased by 22.0 ± 11.5% ($P = 0.04$; $n = 11$) during inspiration and by 113.6 ± 42.9% during expiration compared to pre-injection values ($P = 0.01$; $n = 11$).

In four out of the eleven experiments, medial injections increased $\int ABD_{EMG}$ activity, while in the remaining seven experiments $ABD_{EMG}$ did not display significant recruitment. Overall, $ABD_{EMG}$ activity was not significantly increased during inspiration (+6.0 ± 5.1%; $P = 0.13$; $n = 11$) or during expiration (+46.1 ± 30.9%; $P = 0.08$; $n = 11$) compared to pre-injection values. Figure 8*A* indicates the core location of the injection sites for these experiments and summarizes the comparison between medial and lateral injections. The region of spread of the fluorescent beads injected with the drug solution was ∼250 μm in diameter, at 2.5 mm from the midline, with the rostrocaudal extent of the injection ranging from 50 ± 9.53 μm caudal of the caudal tip of the facial nucleus to 227.28 ± 26.42 μm rostral of the caudal tip of the FN. No overlap between the two injection sites was observed.

## Discussion

This study investigated the effect of cholinergic receptor activation on pFRG activity and consequent generation of expiratory $ABD_{EMG}$ activity and active expiration. We demonstrated that cholinergic fibres and terminals are present in the area surrounding the facial nucleus and that stimulation of cholinergic receptors (by either CCh or PHYSO local application) activated late expiratory pFRG neurons, potentiated respiration and promoted generation of long lasting active expiration. This effect was not associated with a generalized brain state activation. In addition, we demonstrated that this effect could be blocked by local application of the wide spectrum muscarinic antagonist SCOP and was strongly depressed by M3-preferring muscarinic receptor antagonists. Further, we demonstrated a distinct respiratory response between CCh injection in the region medial to the facial nucleus (corresponding to the previously identified RTN chemosensitive neurons) and the region lateral to the facial nucleus (corresponding to the key expiratory rhythm generating area of the pFRG), further supporting the hypothesis that two specific regions are responsible for distinct respiratory function.

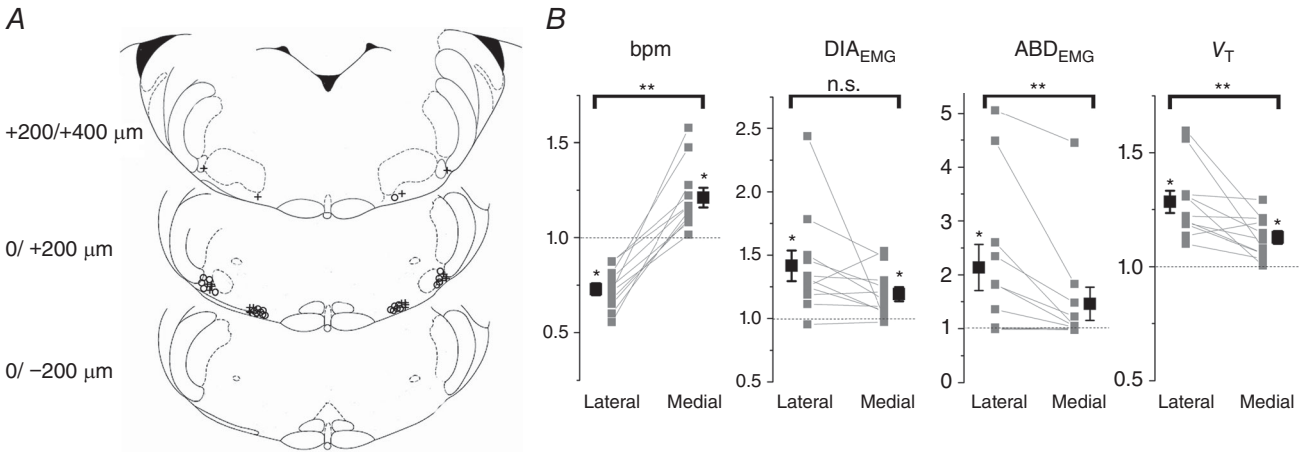


**Figure 8. Local application of carbachol (CCh, 1 mm, 50–100 nl) in the region lateral or medial to the facial nucleus induces different respiratory responses**
*A*, representative sections of adult rat brainstem (modified from Paxinos and Watson, 1998) indicating location of medial and lateral injection sites along the rostro-caudal axis. 0 corresponds to the caudal tip of facial nucleus (VII). Each symbol represents an injection site. Open circles identify injections sites where strong abdominal muscle recruitment was observed. Crosses indicate injection sites that did not elicit ABD recruitment. *B*, summary plots indicating changes in respiratory rate (bpm), peak $\int DIA_{EMG}$ and $\int ABD_{EMG}$ activity, and tidal volume ($V_T$) (relative to pre-injection values (grey, individual experiments; black, averaged data). Connecting lines indicate differential responses across sites in the same rat. *Significant change upon CCh injection compared to pre-injection values; **significant changes between lateral and medial injections ($P < 0.05$). n.s., not significant.

Acetylcholine has been implicated in several aspects of the neural control of respiration, such as respiratory frequency and motor output (Burton *et al.* 1994; Shao & Feldman, 2009), state-dependent modulation of breathing (Kubin & Fenik, 2004), and central and peripheral chemosensitivity, being an important neurotransmitter in the carotid bodies (Nurse, 2010) and having a stimulatory effect on central chemoreceptors (Dev & Loeschcke, 1979; Fukuda & Loeschcke, 1979; Loeschcke, 1982; Gillis *et al.* 1988; Nattie & Li, 1990; Sobrinho *et al.* 2016). Anatomical evidence also suggests that cholinergic innervation is present in the brainstem reticular formation with the majority of cholinergic inputs deriving from the pontine structures of the pedunculopontine tegmental nucleus and the laterodorsal tegmental nucleus (Woolf & Butcher, 1989; Jones, 1990; Woolf, 1991; Yeomans, 2012). An additional source of cholinergic innervation derives from local cholinergic neurons present in the reticular formation (Jones, 1990; Woolf, 1991). Stimulation of mesopontine structures elicits multiple and diverse respiratory responses with occurrence of apnoeas, tachypnoea, EMG depression or activation depending on the site of stimulation within these structures (Topchiy *et al.* 2010). In addition activation of some of the descending projections to the oral pontine nucleus and subceruleus reproduce theta rhythms and muscles atonia observed during REM sleep with diverse respiratory and cortical effects depending on the site of stimulation (Kubin & Fenik, 2004), thus suggesting a complex role of mesopontine structures on respiratory modulation across brain states.

Consistent with this idea, we could identify labelling of cholinergic fibres in the pFRG region and the presence of several cholinergic terminals in neurons located lateral to the facial nucleus (the target area of our pFRG microinjections), as demonstrated by our immunohistochemical data. We conclude that cholinergic fibres run and send synaptic contact to neurons located in the pFRG area. The source of this cholinergic innervation is currently unknown.

Recent evidence from our laboratory shows that spontaneous recruitment of $ABD_{EMG}$ activity often occurs during REM sleep and REM-like states under urethane anaesthesia (Pagliardini *et al.* 2012; Andrews & Pagliardini, 2015). During REM epochs, expiratory $ABD_{EMG}$ recruitment is associated with reduced respiratory variability and an increased tidal volume and minute ventilation compared to respiratory events preceding $ABD_{EMG}$ recruitment. We therefore hypothesized that cholinergic neurotransmission, which is particularly active during REM sleep (McCarley, 2007; Boucetta *et al.* 2014) and REM-like sleep states under urethane anaesthesia (Boucetta & Jones, 2009), may be involved in the recruitment of expiratory ABD muscles through release of acetylcholine in the pFRG region, a key site for providing rhythmic excitatory drive to expiratory muscles. Consistent with this idea, local application of CCh into the pFRG induced strong and long lasting recruitment of active expiration associated with a decrease in breathing rate, activation of $ABD_{EMG}$ muscles, and consequent increase in tidal volume and minute ventilation. Blocking of acetylcholinesterase activity by means of PHYSO promoted gradual recruitment of ABD muscle activity until active expiration was fully developed, suggesting that an increase in endogenous ACh concentration in the pFRG is sufficient to generate active expiration. In conjunction with recruitment of active expiration, we also observed potentiation of DIA and GG inspiratory activity, which may be promoted by a stimulatory effect of pFRG neurons on preBötC or inspiratory premotoneurons (Pagliardini *et al.* 2011), even before full active expiration is developed.

We further tested the hypothesis that muscarinic receptors are involved in this pathway and were able to block CCh-mediated respiratory response by local pre-application of the muscarinic receptor antagonist SCOP. Scopolamine application did not affect ongoing ventilatory properties, similar to the observed effects of local inhibition of pFRG neurons in the resting condition (Huckstepp *et al.* 2015). Interestingly, when expiratory related $ABD_{EMG}$ activity was present prior to SCOP injection, this activity was reduced by SCOP, demonstrating that endogenous release of acetylcholine possibly influences expiratory modulated activity in pFRG of urethane anaesthetized rats. Scopolamine successfully blocked response to CCh until the drug washed out and the CCh-mediated response was consequently recovered. Even though we cannot exclude a contribution of nicotinic neurotransmission to pFRG modulation, our results with scopolamine strongly support a muscarinic mechanism for CCh-mediated pFRG activation. To further test for specific subtype of muscarinic receptors involved in the CCh-mediated pFRG activation, we used more selective antagonists for blocking M1, M2 and M3 receptor subtypes since they have been reported to be present in the respiratory networks in the medulla (Nattie & Li, 1990; Mallios *et al.* 1995; Muere *et al.* 2015): our results suggest that activation of pFRG by CCh is most likely to be mediated by M3 muscarinic receptors.

It is interesting to observe that the excitatory cholinergic effect on expiratory ABD motoneurons is distinct from what was observed in genioglossus and postural muscles when either cholinergic neurotransmission is locally modulated (Grace *et al.* 2013) or PPT area is locally stimulated with CCh in an animal model of sleep (Kubin & Fenik, 2004). While both phenomena also occur in natural sleep (i.e. genioglossus and postural muscle activity are depressed; reviewed in Chase & Morales, 1990; ABD muscles are activated; Andrews & Pagliardini, 2015), the mechanisms through which they occur may be different.

It is well known that the majority of postural muscles are depressed during REM sleep. This may be due to active inhibition promoted by either GABA or glycine (Peever, 2011) or by active inhibitory mechanisms that may use acetylcholine as the major neurotransmitter (Grace *et al.* 2013). Despite this general inhibition, other muscles either maintain their activity (diaphragm) or are activated during periods of REM sleep. We propose that ABD muscles, at least in rodents, are recruited during periods of REM sleep and this activation may be mediated by cholinergic transmission at the level of the expiratory oscillator, the pFRG. Activation of the oscillator, located in the pFRG, is likely to have activated pre-motoneurons in the caudal ventral respiratory group (or nucleus retroambiguus) that eventually send a rhythmic excitatory drive to the abdominal motoneurons located in low thoracic, high lumbar levels of the spinal cord (Janczewski *et al.* 2002; Boers *et al.* 2006; Janczewski & Feldman, 2006; Giraudin *et al.* 2008; Huckstepp *et al.* 2016).

Recent data support the hypothesis that pFRG neurons located lateral to the facial nucleus in the ventral medulla are important for expiratory rhythm generation and are functionally distinct from the more medially located chemosensitive RTN neurons (Abbott *et al.* 2011; Pagliardini *et al.* 2011; Huckstepp *et al.* 2015). Local optogenetic stimulation or release of inhibition within this region activates pFRG neurons with a late expiratory activity and promote recruitment of $ABD_{EMG}$ activity and active expiration (Pagliardini *et al.* 2011). Further, optogenetic stimulation of pFRG neurons affects breathing rhythms by resetting ongoing inspiratory activity (Pagliardini *et al.* 2011). Distinct respiratory effects were obtained when the more medial Phox2b-expressing chemosensitive RTN neurons were stimulated (Abbott *et al.* 2011).

Furthermore, acute silencing of either the lateral pFRG region or the medial RTN region in both the resting condition and under an increased respiratory drive (hypoxia or hypercapnia) induced distinct respiratory responses (Huckstepp *et al.* 2015). The different respiratory responses to neuronal inhibition support the hypothesis that the medial (i.e. RTN) and lateral (i.e. pFRG) parafacial region have a distinct role in respiratory control. Our current results provide further evidence for this hypothesis by demonstrating that cholinergic stimulation of the two sites (medial and lateral) elicits distinct responses in respiratory frequency, tidal volume and ABD recruitment. In this set of experiments we used smaller volumes and lower CCh concentration, in order to avoid spread of drug into the site of comparison and to better evaluate the site of injection. It is therefore not surprising that not all of the experiments provided an intense response in terms of $ABD_{EMG}$ recruitment, as the excitation was potentially not sufficient to drive the activity of the expiratory oscillatory network. In this regard, we observed some $ABD_{EMG}$ recruitment upon medial injections; this may be due to (i) unwanted spread of the drug lateral to the facial nucleus, (ii) the presence of some expiratory oscillator neurons in the medial region, or (iii) more likely, indirect activation of pFRG neurons via RTN activation. We believe that the latter hypothesis is most likely since previous work has demonstrated the important role of Phox2b-expressing chemosensitive RTN neurons in providing a tonic drive to both inspiratory and expiratory activity (Abbott *et al.* 2009; Marina *et al.* 2010; Abbott *et al.* 2011). Nonetheless, changes in respiratory frequency upon CCh injections are indicative of a differential response to CCh for the two sites. The depression in breathing occurring upon lateral (pFRG) injection is consistent with the reported effects occurring upon release of inhibition with GABAergic and glycinergic antagonists and consequent activation of pFRG neurons (Pagliardini *et al.* 2011; Huckstepp *et al.* 2015). The cellular and network mechanisms associated with a reduced respiratory rate during ongoing pFRG activation are not yet clear. One possibility is that pFRG neurons interact with preBötC neurons to reduce respiratory rate. On the other hand, the small but significant increase in respiratory rate upon CCh injection is likely to be driven by the preBötC through excitation provided by RTN neurons (Abbott *et al.* 2009, 2011).

We conclude that cholinergic innervation is present in the pFRG area, and likely to act through muscarininc receptors that depolarize and activate rhythmic pFRG neurons. The source of cholinergic innervation is currently unknown. Pedunculopontine tegmental and laterodorsal tegmental nuclei are the most likely candidates since they contain cholinergic neurons, are active in REM epochs and have been shown to project to the reticular formation (Woolf & Butcher, 1989; Jones, 1990). Pre- or post-synaptic muscarinic receptors may be involved in the process as cholinergic fibres and terminals are present in the area of pFRG. Further studies will be necessary to investigate the presence of direct cholinergic projections to pFRG neurons in order to determine the correlation between REM active structures, rhythmic activation of pFRG neurons, and expression of active recruitment of expiratory ABD muscles.

## References

Abbott SB, Stornetta RL, Coates MB & Guyenet PG (2011). Phox2b-expressing neurons of the parafacial region regulate breathing rate, inspiration, and expiration in conscious rats. *J Neurosci* **31**, 16410–16422.

Abbott SB, Stornetta RL, Fortuna MG, Depuy SD, West GH, Harris TE & Guyenet PG (2009). Photostimulation of retrotrapezoid nucleus phox2b-expressing neurons in vivo produces long-lasting activation of breathing in rats. *J Neurosci* **29**, 5806–5819.

Andrews CG & Pagliardini S (2015). Expiratory activation of abdominal muscle is associated with improved respiratory stability and an increase in minute ventilation in REM epochs of adult rats. *J Appl Physiol* **119**, 968–974.

Boers J, Kirkwood PA, de Weerd H & Holstege G (2006). Ultrastructural evidence for direct excitatory retroambiguus projections to cutaneous trunci and abdominal external oblique muscle motoneurons in the cat. *Brain Res Bull* **68**, 249–256.

Boucetta S, Cisse Y, Mainville L, Morales M & Jones BE (2014). Discharge profiles across the sleep-waking cycle of identified cholinergic, GABAergic, and glutamatergic neurons in the pontomesencephalic tegmentum of the rat. *J Neurosci* **34**, 4708–4727.

Boucetta S & Jones BE (2009). Activity profiles of cholinergic and intermingled GABAergic and putative glutamatergic neurons in the pontomesencephalic tegmentum of urethane-anesthetized rats. *J Neurosci* **29**, 4664–4674.

Burke PG, Kanbar R, Basting TM, Hodges WM, Viar KE, Stornetta RL & Guyenet PG (2015). State-dependent control of breathing by the retrotrapezoid nucleus. *J Physiol* **593**, 2909–2926.

Burton MD, Nouri K, Baichoo S, Samuels-Toyloy N & Kazemi H (1994). Ventilatory output and acetylcholine: perturbations in release and muscarinic receptor activation. *J Appl Physiol* **77**, 2275–2284.

Chase MH & Morales FR (1990). The atonia and myoclonia of active (REM) sleep. *Annu Rev Psychol* **41**, 557–584.

Dev NB & Loeschcke HH (1979). A cholinergic mechanism involved in the respiratory chemosensitivity of the medulla oblongata in the cat. *Pflugers Arch* **379**, 29–36.

Feldman JL, Del Negro CA & Gray PA (2013). Understanding the rhythm of breathing: so near, yet so far. *Annu Rev Physiol* **75**, 423–452.

Fukuda Y & Loeschcke HH (1979). A cholinergic mechanism involved in the neuronal excitation by $H^+$ in the respiratory chemosensitive structures of the ventral medulla oblongata of rats in vitro. *Pflugers Arch* **379**, 125–135.

Gillis RA, Walton DP, Quest JA, Namath IJ, Hamosh P & Dretchen KL (1988). Cardiorespiratory effects produced by activation of cholinergic muscarinic receptors on the ventral surface of the medulla. *J Pharmacol Exp Ther* **247**, 765–773.

Giraudin A, Cabirol-Pol MJ, Simmers J & Morin D (2008). Intercostal and abdominal respiratory motoneurons in the neonatal rat spinal cord: spatiotemporal organization and responses to limb afferent stimulation. *J Neurophysiol* **99**, 2626–2640.

Gourine AV, Kasymov V, Marina N, Tang F, Figueiredo MF, Lane S, Teschemacher AG, Spyer KM, Deisseroth K & Kasparov S (2010). Astrocytes control breathing through pH-dependent release of ATP. *Science* **329**, 571–575.

Grace KP, Hughes SW & Horner RL (2013). Identification of the mechanism mediating genioglossus muscle suppression in REM sleep. *Am J Respir Crit Care Med* **187**, 311–319.

Grundy D (2015). Principles and standards for reporting animal experiments in *The Journal of Physiology* and *Experimental Physiology*. *J Physiol* **593**, 2547–2549.

Guyenet PG & Bayliss DA (2015). Neural control of breathing and $CO_2$ homeostasis. *Neuron* **87**, 946–961.

Huckstepp RT, Cardoza KP, Henderson LE & Feldman JL (2015). Role of parafacial nuclei in control of breathing in adult rats. *J Neurosci* **35**, 1052–1067.

Huckstepp RT, Henderson LE, Cardoza KP & Feldman JL (2016). Interactions between respiratory oscillators in adult rats. *Elife* **5**, e14203.

Janczewski WA & Feldman JL (2006). Distinct rhythm generators for inspiration and expiration in the juvenile rat. *J Physiol* **570**, 407–420.

Janczewski WA, Onimaru H, Homma I & Feldman JL (2002). Opioid-resistant respiratory pathway from the preinspiratory neurones to abdominal muscles: in vivo and in vitro study in the newborn rat. *J Physiol* **545**, 1017–1026.

Jones BE (1990). Immunohistochemical study of choline acetyltransferase-immunoreactive processes and cells innervating the pontomedullary reticular formation in the rat. *J Comp Neurol* **295**, 485–514.

Kodama T, Lai YY & Siegel JM (1992). Enhancement of acetylcholine release during REM sleep in the caudomedial medulla as measured by in vivo microdialysis. *Brain Res* **580**, 348–350.

Kubin L & Fenik V (2004). Pontine cholinergic mechanisms and their impact on respiratory regulation. *Respir Physiol Neurobiol* **143**, 235–249.

Loeschcke HH (1982). Central chemosensitivity and the reaction theory. *J Physiol* **332**, 1–24.

Mallios VJ, Lydic R & Baghdoyan HA (1995). Muscarinic receptor subtypes are differentially distributed across brain stem respiratory nuclei. *Am J Physiol Lung Cell Mol Physiol* **268**, L941–L949.

Marina N, Abdala AP, Trapp S, Li A, Nattie EE, Hewinson J, Smith JC, Paton JF & Gourine AV (2010). Essential role of Phox2b-expressing ventrolateral brainstem neurons in the chemosensory control of inspiration and expiration. *J Neurosci* **30**, 12466–12473.

McCarley RW (2007). Neurobiology of REM and NREM sleep. *Sleep Med* **8**, 302–330.

Mellen NM, Janczewski WA, Bocchiaro CM & Feldman JL (2003). Opioid-induced quantal slowing reveals dual networks for respiratory rhythm generation. *Neuron* **37**, 821–826.

Muere C, Neumueller S, Miller J, Olesiak S, Hodges MR, Pan L & Forster HV (2015). Evidence for respiratory neuromodulator interdependence after cholinergic disruption in the ventral respiratory column. *Respir Physiol Neurobiol* **205**, 7–15.

Nattie EE & Li AH (1990). Ventral medulla sites of muscarinic receptor subtypes involved in cardiorespiratory control. *J Appl Physiol* **69**, 33–41.

Nurse CA (2010). Neurotransmitter and neuromodulatory mechanisms at peripheral arterial chemoreceptors. *Exp Physiol* **95**, 657–667.

Pagliardini S, Gosgnach S & Dickson CT (2013). Spontaneous sleep-like brain state alternations and breathing characteristics in urethane anesthetized mice. *PLoS One* **8**, e70411.

Pagliardini S, Greer JJ, Funk GD & Dickson CT (2012). State-dependent modulation of breathing in urethane-anesthetized rats. *J Neurosci* **32**, 11259–11270.

Pagliardini S, Janczewski WA, Tan W, Dickson CT, Deisseroth K & Feldman JL (2011). Active expiration induced by excitation of ventral medulla in adult anesthetized rats. *J Neurosci* **31**, 2895–2905.

Pagliardini S, Ren J & Greer JJ (2003). Ontogeny of the pre-Botzinger complex in perinatal rats. *J Neurosci* **23**, 9575–9584.

Peever J (2011). Control of motoneuron function and muscle tone during REM sleep, REM sleep behavior disorder and cataplexy/narcolepsy. *Arch Ital Biol* **149**, 454–466.

Paxinos G & Watson C (1998). The rat brain in stereotaxic coordinates, 4th Edition. New York: Academic Press.

Shao XM & Feldman JL (2009). Central cholinergic regulation of respiration: nicotinic receptors. *Acta Pharmacol Sin* **30**, 761–770.

Smith JC, Ellenberger HH, Ballanyi K, Richter DW & Feldman JL (1991). Pre-Botzinger complex: a brainstem region that may generate respiratory rhythm in mammals. *Science* **254**, 726–729.

Sobrinho CR, Kuo F-S, Barna BF, Moreira TS & Mulkey DK (2016). Cholinergic control of ventral surface chemoreceptors involves Gq/inositol 1,4,5-trisphosphate-mediated inhibition of KCNQ channels. *J Physiol* **594**, 407–419.

Topchiy I, Waxman J, Radulovacki M & Carley DW (2010). Functional topography of respiratory, cardiovascular and pontine-wave responses to glutamate microstimulation of the pedunculopontine tegmentum of the rat. *Respir Physiol Neurobiol* **173**, 64–70.

Woolf NJ (1991). Cholinergic systems in mammalian brain and spinal cord. *Prog Neurobiol* **37**, 475–524.

Woolf NJ & Butcher LL (1989). Cholinergic systems in the rat brain: IV. Descending projections of the pontomesencephalic tegmentum. *Brain Res Bull* **23**, 519–540.

Yeomans JS (2012). Muscarinic receptors in brain stem and mesopontine cholinergic arousal functions. *Handb Exp Pharmacol*, 243–259.

## Additional information

### Competing interests

None declared.

### Author contributions

All authors have approved the final version of the manuscript and agree to be accountable for all aspects of the work. All persons designated as authors qualify for authorship, and all those who qualify for authorship are listed. The experiments were conducted entirely in the Pagliardini laboratory at the University of Alberta. SP was responsible for conception and experimental design. RCTB, ZA and SP contributed to the acquisition, analysis, and interpretation of data; RCTB, ZA and SP wrote the manuscript.

### Funding

This research was funded by an NSERC Discovery Grant (S.P.) and WCHRI recruitment grant (S.P.); R.B. was funded by an NSERC undergraduate summer research studentship. Z.A. is the recipient of a studentship from King Saud Bin Abdulaziz University for Health Sciences College of Medicine (Saudi Arabia).